# Signal simulations in urban environments

A. Steingass[1], B. Krach[1], F. Schubert[1] and M. Crisci[2], R. Prieto-Cerdeira[2]

[1]*German Aerospace Center (DLR), Institute of Communications and Navigation, Germany*
[2]*European Space Agency (ESA), the Netherlands*

## BIOGRAPHY

Dr. Alexander Steingass received his degree in electrical engineering from University of Ulm, Germany in 1996. Since 1997 he is with the German Aerospace Centre (DLR), Institute for Communications and Navigation. He received his Phd. from University of Essen. His major fields of work are: digital signal processing, multipath propagation and signal and system design in particular with GNSS systems. He actively participates in ITU-R Study Group 3 and has been awarded with "Innovation award EEEFCOM" 2007, the ION best presentation award 2003 and 2010 for this paper.

Frank Schubert received his Diploma degree 2007 in Electrical Engineering and Information Technology from the University of Karlsruhe. Since 2007 he is member of the scientific staff of the Institute for Communications and Navigation of the German Aerospace Center (DLR). Since October 2007 he is participating in the ESA Networking / Partnering Initiative (NPI). In his pursuit of a PhD degree he is also embedded in the NavCom section at the University of Aalborg, Denmark. His research topics comprise modelling of the non-stationary GNSS channel and the time-domain simulation of modern GNSS algorithms. Frank received the Best Presentation Award in 2009, he is a regional winner of the European Satellite Navigation Competition (Galileo Masters) 2009 and he was the leader of the winning team of the Student Project Work Competition of the 2nd Int'l GNSS Summer School 2008 in Berchtesgaden, Germany.

Dr. Bernhard Krach received a diploma and a doctoral degree in electrical engineering both from University of Erlangen-Nuremberg, Germany, in 2005 and 2009, respectively. From 2005 to 2009 he has been with the Institute of Communications and Navigation at the German Aerospace Center (DLR), Oberpfaffenhofen, Germany. In 2009 he joined EADS Cassidian Air Systems, Manching, Germany.

Roberto Prieto-Cerdeira received his Telecommunications Engineering degree from the University of Vigo, Spain in 2002 and followed postgraduate studies on Space Science and Radioastronomy in Chalmers University of Technology (Gothenburg, Sweden). Since 2004, he has been with the European Space Agency (ESA/ESTEC), Noordwijk, The Netherlands in the Electromagnetics and Space Environment Division where he is responsible of the activities related to radiowave propagation in the ionosphere and local environment in particular for Global Navigation Satellite Systems (GNSS), such as Galileo and EGNOS projects, and Satellite Mobile Communications. He actively participates in ITU-R Study Group 3, COST IC0802, SBAS-Iono group and the Network of Experts on Electromagnetic Wave Propagation (NoE-EWP).

Dr. Massimo Crisci has a Ph.D. in Automatics and a Master's degree in Electronics Engineering. He is the Head of the Navigation Section under the technical Department in ESA (TEC/ETN), which provides technical expertise to the ESA Navigation programs and leads various research projects. Previously working as Radio Navigation and Signal Processing Engineer, part of the GALILEO/GIOVE System/GMS engineering team, he is in charge of the procurement of the GALILEO Receiver Chain PRS and Non-PRS for the Ground Mission Segment and various other R&D activities.

## ABSTRACT

In this paper we use a realistic channel model (ITU-R 681-7) to realistically simulate multipath and fading conditions in an urban environment. From these simulations we have found three major conclusions:

The receiver performance is very dependent on the used signal in space. It turns out that for this difficult environment the narrow band signals such as GPS C/A and BOC (1,1) can be robustly tracked by the receivers while the wideband signals such as GPS L2, L5, GALILEO E5b, and E5 are causing the loss of tracking. This behavior can be explained by the fact, that the wideband signals are designed suppress multipath components of the signal. If the LOS is then shadowed too little signal power is left to track these signals. Furthermore it can be seen that BOC (1,1) clearly outperforms the GPS C/A signal.

A comparison of different receivers has been carried out: A classical narrow correlation DLL, a DLL using a

double delta correlator, a multipath estimating DLL and a particle filter based receiver have been compared. In this difficult environment the particle filter receiver showed the best performance followed by the MEDLL and the classical DLLs.

Last but not least a critical situation for a DLL receiver has been envisaged: The "short line of sight hit" (SLOSH) – a situation where the receiver is faced wit a LOS with a short duration after a shadowing period can mislead the DLLs integrators and cause a loss of lock.

## INTRODUCTION

In the last years a lot of simulations concerning the performance analysis of new signal alternatives have been carried out. Most of these analysis assume a AWGN channel for the simulation. This assumption might be useful for unobstructed situations where multipath is mitigated by the antenna but seems not be feasible for urban environments.
This lack of knowledge about the performance of new signals in realistic urban environments was the motivation to reenter this topic with a realistic channel model. We have selected the land mobile model ITU-R 681-7 as a realistic replica of the urban environment for this paper.

## THE CHANNEL MODEL USED

In 2002 we have performed extensive measurements on the multipath channel [6]. From these measurements we have developed a realistic channel model which has been published in [7] and later be standardized by ITU 681-7. In the following section we will briefly describe the model but for more details we refer to [7].

### Direct Path

In an open environment the direct path would be best represented by the line of sight (LOS) transmission of the signal. In an urban environment this LOS signal is often blocked so that the first received path is attenuated and possibly delayed with respect to the LOS. In cities we had been able to identify three major types of obstacles that influence the signal reception.

- House fronts
- Trees
- Lampposts

### Reflected signal

In the measurement data many reflections appear in the urban environment. In contrast to ray tracing algorithms we do not model a specific scenery. We assume reflections to be statistically distributed in the x,y,z space and generate them statistically. In order to match the measured statistic we must take a closer look at the echo distribution.

### Geometric occurrence of reflectors

**Figure 1** shows the likelihood distribution of reflectors in a top view. In this figure the receiver is moving in x-direction only. It can clearly be seen that the highest likelihood of receiving a reflector is when the reflector is on the right or on the left side. The likelihood of receiving a reflector from the front is close to zero. This as well on the first look astonishing result becomes more plausible when one has an urban canyon in mind. It must be unlikely that a reflecting obstacle is in near front position of the car, otherwise one would overrun it in the next second. The conditional likelihood of a reflector being present at a certain position for a specific satellite azimuth is calculated from the statistics. The result is shown in **Figure 2**, here the satellite position had been chosen at 25° azimuth.

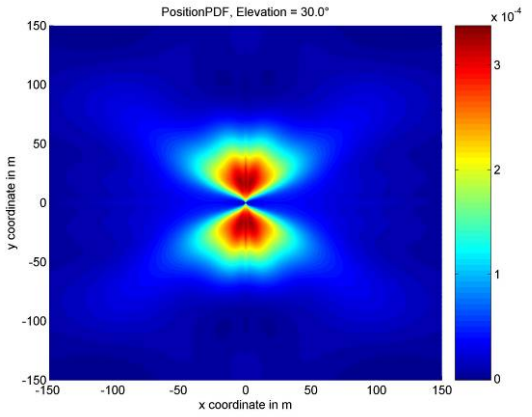


**Figure 1: Likelihood of reflectors being at a certain 2-D position. Moving direction of the receiver is in x-direction only.**

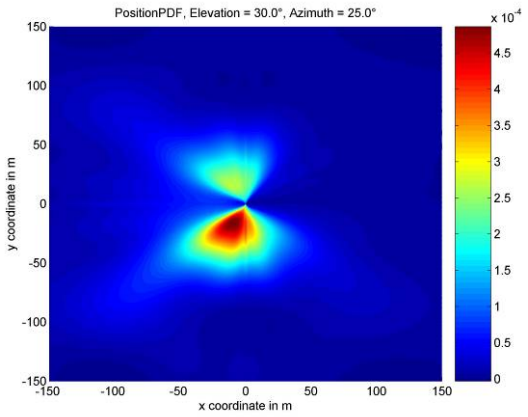


**Figure 2: Conditional likelihood of reflectors being at a certain 2-D position. Satellite at 25° azimuth.**

#### Lifespan of reflectors

In the measurement data the channel appears rapidly changing. Many echoes disappear and others appear at new positions. This process is highly correlated to the receiver speed. When the car stops the reflections

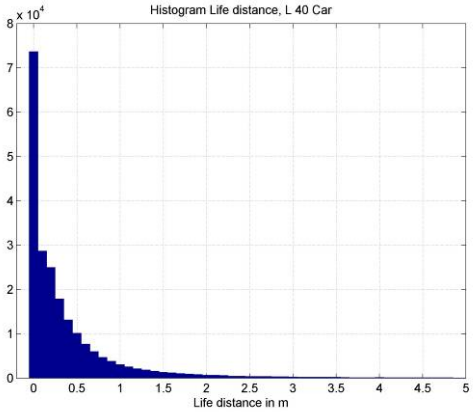


**Figure 3: Live distance of echoes**

remain in the scenery. Therefore we defined a life distance of each reflector. This life distance is the distance the receiver is travelling until the echo disappears. **Figure 3** shows a histogram of the echo life distances. It can be seen that the life distance of the reflectors is usually well below 1 m. Most reflectors exist along a motion path below 5 m. Therefore the channel is changing rapidly.

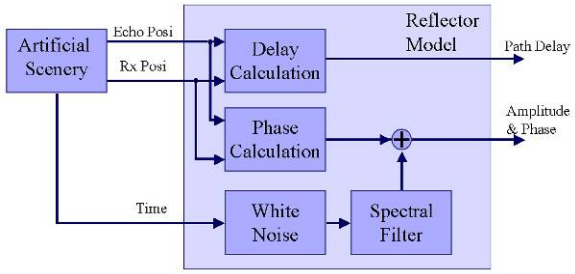


**Figure 4: Model of an isolated reflector**

**Figure 4** shows how a single reflector is modelled. In terms of the reflector the artificial scenery generates a continues series of receiver positions according to the actual speed. The receiver is moving only in x-direction. To simulate turns the relative azimuth of the satellite is changed.

#### Number of echoes

During a drive through a city the number of echoes being received changes. For a navigation receiver that tries to estimate the channel impulse response (super resolution for multipath mitigation) a high number of reflections is a ”high stress scenario”. Other phases with a lower number of echoes are less critical. Besides the mean number of echoes it is therefore very important to exactly model this increasing and decreasing process. A sample of it is shown in **Figure 5**. Please note the relatively high number of echoes (up to 50) at the same time. We had been able to detect two processes: An extremely narrow band process with high power and a lower powered wide band process. Their combination results in a very good approximation of the process.

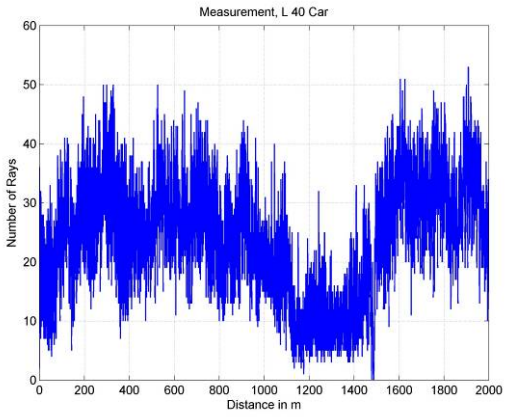


**Figure 5: Number of echoes at the same time during a 15 min drive trough a city.**

The block diagram in **Figure 6** gives an overview of the implemented model. The x-coordinate and the relative satellite azimuth are derived from the user speed, user heading and satellite azimuth as explained in section 4.6. This drives the artificial scenery (**Figure 7**) where house fronts, trees and lampposts affect the direct path. Controlled by a number of echo

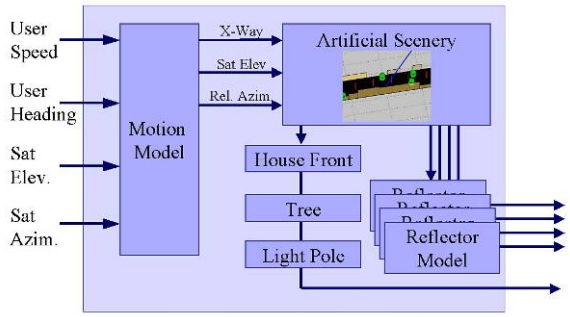


**Figure 6: Block diagram of the channel model.**

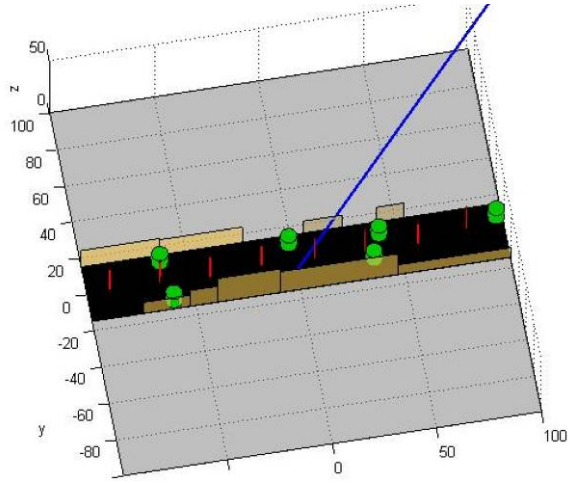


**Figure 7: A picture of the artificial scenery. Brown are house fronts, green cylinders are trees, red are poles.**

generator the actual amount of reflections is created in the scenery at positions according to the likelihood distribution. The reflectors power, bandwidth, rice factor and lifespan are taken from the statistics. Their delay and phase is therefore changing according to this statistical parameters and according to the receiver movement relative to the reflector position. In **Figure 8 - Figure 11** an example output of the channel model is given. In this scenario the car drove with a variable speed (using a sin(t) like stop and go function) through the city. At 4.7 s the speed of the vehicle was nearly 0 km/h. In **Figure 9** the Doppler shift of every echo is shown. The red dotted line is the theoretical limit for the Doppler shift given by

$$f_{Doppler} = \frac{\vec{v} \cdot \left(\overrightarrow{RX} - \vec{S}\right)}{c_0} f_C \qquad (4)$$

where v is the speed vector of the vehicle, RX is the receiver position, fC is the carrier frequency, S is the satellite Position and c0 is the speed of light. In this figure and in the detail (**Figure 11**) one can determine isolated echoes changing their Doppler shift during their life distance (for example the mint green colored echo lasting from 0.81 - 1.35 s). The rapid changes in the channel are visible within the displayed period of around one second many echoes die and others are generated. Around the standstill the channel does not

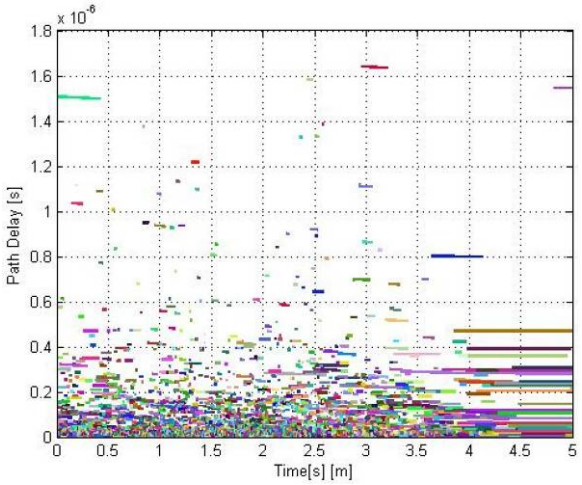


**Figure 8: Example of generated echoes. Plotted is the path delay of the reflections over time.**

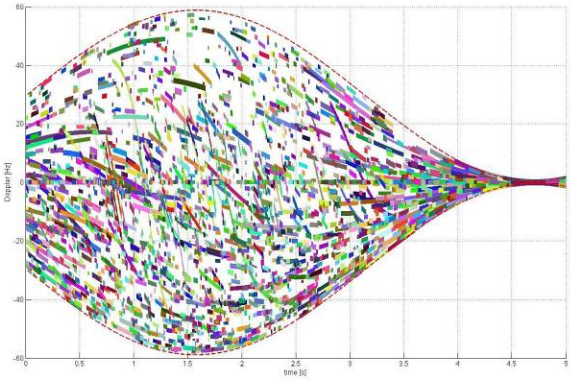

**Figure 9: Example of generated echoes. Plotted is the Doppler of the reflections over time.**

change much - clearly visible by the low Doppler bandwidth and the long lasting echoes (long lines) in **Figure 8**. In this situation only the time driven fading process is changing the channel. But neither an echo is terminated nor a new one is generated in this situation. Furthermore one can see regions where more echoes are present than in others. Due to this precise modelling of reflections new receiver algorithms for e.g. multipath mitigation can be tested in very realistic simulations now. An important improvement compared to regular statistical models is the geometrical reflector representation which guarantees the realistic delay and phase correlation among the occurring echoes.

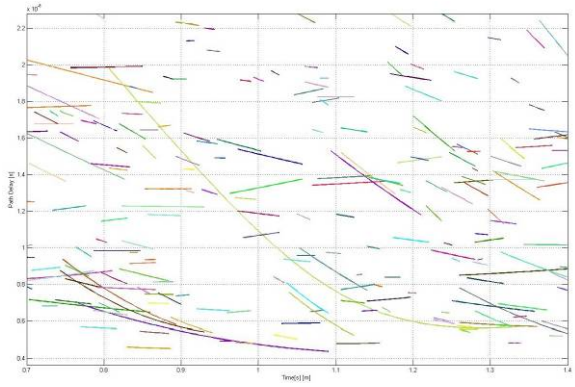

**Figure 10: Detail of Figure 8.**

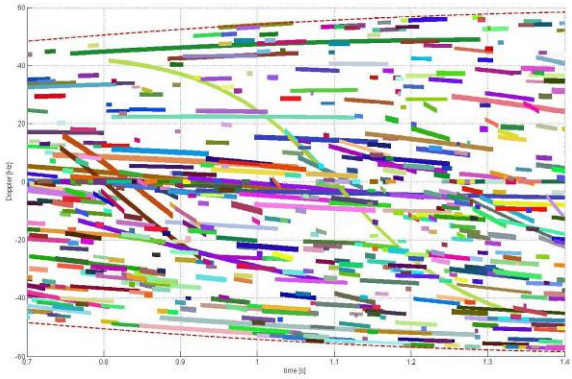

**Figure 11: Detail of Figure 9.**

## RECEIVERS AND MULTIPATH MITIGATION

Multipath is today still one of the most crucial problems in GNSS, as the error is caused locally and can not be corrected through the use of correction data, which is provided by reference receiver stations or networks. The advances in the development of signal processing techniques for multipath mitigation have led to continuous improvements over the past decades, whereas basically two major approaches can be distinguished: First, the class of techniques that actually mitigate the effect of multipath by aligning the more or less traditional receiver components (see Figure 1). Most of these conventional mitigation techniques are in some way aligning the discriminator of the delay lock loop (DLL) to the signal received in the multipath environment. Well-known examples of this category are the Narrow Correlator [1] and the Strobe Correlator [2].

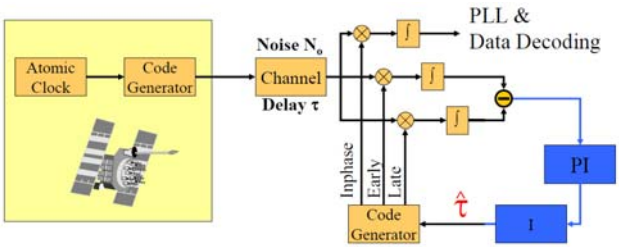


**Figure 12: Signal generation, signal propagation through the channel, and signal reception with a DLL receiver.**

Second, the class of multipath estimation techniques, which treat multipath, i.e. specifically the delays of the paths, as something to be estimated from the received signal, so that its effects can be trivially removed at a later processing stage. For the estimation techniques static and dynamic approaches can be distinguished, according to the underlying assumption of the channel dynamics. Examples for static multipath estimation are those belonging to the family of maximum likelihood (ML) estimators, where the probably best-known technique is the multipath estimating delay lock loop (MEDLL) [3]. During the last years sequential estimation algorithms in the form of Bayesian filters have gained some attention in the field of multipath mitigation [4]. These algorithms exploit prior knowledge about the temporal channel statistics through the use of statistical channel models, which allows one to improve the multipath performance of the receiver.

### Multipath Estimation Signal Model

The common fundament of the estimation approaches is to consider the multipath reception explicitly when designing receiver. Hence, in a multipath estimating receiver the complex valued baseband-equivalent received signal is assumed to equal

$$z(t) = \sum_{i=0}^{N_m} a_i s(t-\tau_i) + n(t) \ , \qquad (1)$$

where $s(t)$ is the transmitted navigation signal, $N_m+1$ is the total number of paths reaching the receiver, and $a_i(t)$ and $\tau_i(t)$ are their individual complex amplitudes and time delays, respectively. The signal is disturbed by additive white Gaussian noise $n(t)$ of power $\sigma^2$. Grouping blocks of $L$ samples at times $(n+kL)T_s$, $n$=0,…,$L$-1, together into vectors, and assuming that the delays and amplitudes are

constant and equal to $\boldsymbol{\tau}_k=(\tau_{k,1},\ldots,\tau_{k,Nk})^T$ and $\mathbf{a}_k=(a_{k,0},\ldots,a_{k,Nm})^T$ within the corresponding time interval, the likelihood function for the signal parameter estimation problem is given by the complex normal distribution

$$p(\mathbf{z}_k \mid \boldsymbol{\tau}_k, \mathbf{a}_k) = \mathrm{N}\left( \sum_{i=0}^{N_m} a_{k,i}\mathbf{s}(\tau_{k,i}); \sigma^2 \right) . \qquad (2)$$

**Maximum Likelihood Estimation**

As the naming implies the ML estimate is the set of parameters, which maximizes the likelihood function, i.e. the conditional probability of the received signal:

$$\left\{ \hat{\boldsymbol{\tau}}_k^{\mathrm{ML}}, \hat{\mathbf{a}}_k^{\mathrm{ML}} \right\} = \underset{\boldsymbol{\tau}_k, \mathbf{a}_k \mid N_m}{\arg\max}\, p(\mathbf{z}_k \mid \boldsymbol{\tau}_k, \mathbf{a}_k) . \qquad (3)$$

Since a closed form solution of (3) does not exist, several strategies have been proposed in the literature to implement the estimator, where most of them estimate the amplitudes analytically whereas the delay estimates are obtained iteratively by means of numerical optimization methods. The actual number of received paths $N_m$+1, which is unknown in practice, too, is commonly estimated separately along using a statistical detection test.
For the simulations performed in this paper we solved (3) via a Newton-type method. To estimate the number of paths a likelihood ratio test was implemented.

**Sequential Bayesian Estimation**

In contrast to the ML estimator in a sequential Bayesian estimator the estimates are not obtained independently for each observation interval. Instead at each time step prior knowledge, which is derived from past observation intervals, is used to refine the estimates. Specifically the parameters $\boldsymbol{\tau}_k$ and $\mathbf{a}_k$ are estimated for each time instant $k$ in terms of the a-posteriori probability density function (PDF) $p(\boldsymbol{\tau}_k,\mathbf{a}_k|\mathbf{Z}_k)$, with $\mathbf{Z}_k=\{\mathbf{z}_k,\ldots,\mathbf{z}_0\}$ being the entire history of received measurements up to the time instant $k$. The sequence of a-posteriori PDFs can be computed recursively by alternating calculation of the *prediction step* (via the Chapman-Kolmogorov equation)

$$p(\boldsymbol{\tau}_k, \mathbf{a}_k \mid \mathbf{Z}_{k-1}) = \int p(\boldsymbol{\tau}_k, \mathbf{a}_k \mid \boldsymbol{\tau}_{k-1}, \mathbf{a}_{k-1}) \cdot p(\boldsymbol{\tau}_{k-1}, \mathbf{a}_{k-1} \mid \mathbf{Z}_{k-1}) \mathrm{d}\boldsymbol{\tau}_{k-1} \mathrm{d}\mathbf{a}_{k-1} , \qquad (4)$$

which exploits the statistical dependencies between successive observation intervals through the transition density $p(\boldsymbol{\tau}_k,\mathbf{a}_k|\boldsymbol{\tau}_{k-1},\mathbf{a}_{k-1})$ in order to compute the a-priori PDF, and the computation of the *update step*

$$p(\boldsymbol{\tau}_k, \mathbf{a}_k \mid \mathbf{Z}_k) = \frac{p(\mathbf{z}_k \mid \boldsymbol{\tau}_k, \mathbf{a}_k) p(\boldsymbol{\tau}_k, \mathbf{a}_k \mid \mathbf{Z}_{k-1})}{p(\mathbf{z}_k \mid \mathbf{Z}_{k-1})} , \qquad (5)$$

in which the likelihood function is joined with the previous a-priori PDF. Once this a-posteriori PDF is evaluated, either the channel configuration that maximizes it can be determined – the so-called maximum a-posteriori (MAP) estimate; or the expectation can be choosen – equivalent to the minimum mean square error (MMSE) estimate:

$$\hat{\boldsymbol{\tau}}_k^{\mathrm{MMSE}} = \int \boldsymbol{\tau}_k p(\boldsymbol{\tau}_k, \mathbf{a}_k \mid \mathbf{Z}_k) \mathrm{d}\boldsymbol{\tau}_k \mathrm{d}\mathbf{a}_k . \qquad (6)$$

To implement the sequential Bayesian estimator we employed a marginalized particle filter, in which also the number of received paths was detected and estimated simultaneously. Details on the filter algorithm can be found in [4].

**EVALUATION OF RECEIVERS**

An example to illustrate the capability to suppress multipath by using a particle receiver can be seen in Figure 13. In this situation a car is moving through a city an is receiving a strong LOS and a strong reflection which is occurring constantly in a very constant relative delay to the LOS. The LOS estimate of the NC-DLL (blue) is significantly disturbed due to a strong echo, which arises and persists during the movement of the receiver. In contrast, the LOS estimate of the particle filter (green) remains accurate, since the echo (red) is detected and tracked properly. This explains why the strategy to detect and estimate reflections significantly improves the receiver performance rather than the invention of new correlator types.

A much more severe situation is shown in Figure 14. Here a strong echo is present and the LOS is often shadowed. While in the shadowing situation the classical DLL receiver (blue) is attracted by the echo the particle receiver is estimating the echo (red) which results in a much better performance for the pseudorange estimate (green).

Beside these promising examples a statistical performance evaluation for the assessed receiver types in terms of the cumulative probability density function of the tracking errors is given in Figure 2. Both conventional DLL receivers perform quite similar, however, the ΔΔ-DLL is slightly superior in the range of errors below 20 m. This fact indicates that the improved multipath mitigation capabilities of a ΔΔ-DLL compared to a NC-DLL are indeed exploited, given the DLL is locked properly. Interestingly, the ML-DLL performs worse than the conventional DLLs for smaller errors, but is superior for

larger errors. The poor performance in the range of smaller errors is due to the limited observation time in such fast varying multipath channels. Hence, at each time instant independent estimates are obtained based on short observations of the channel and no use is made of the channel's temporal correlation. The particle receiver overcomes this limitation: Though the channel is varying fast its temporal correlation is exploited by the massive parallel estimation approach of the particle filter, which adaptively detects and tracks multipath replica and thus is able to reduce the multipath induced tracking errors significantly (see Figure 15).

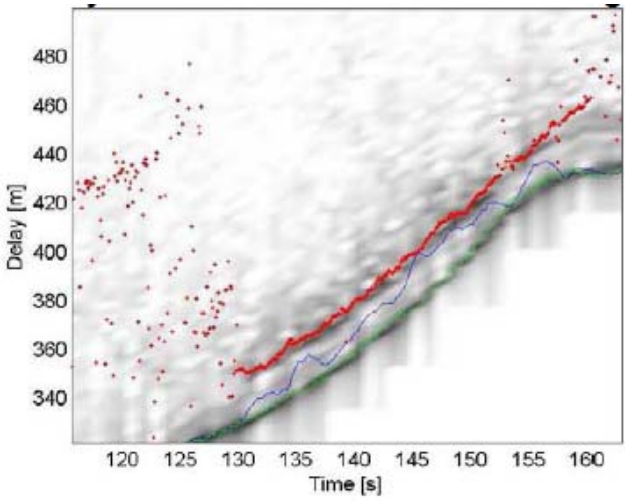


**Figure 13: Direct comparison of particle receiver, and NC-DLL – example: Strong reflection.**

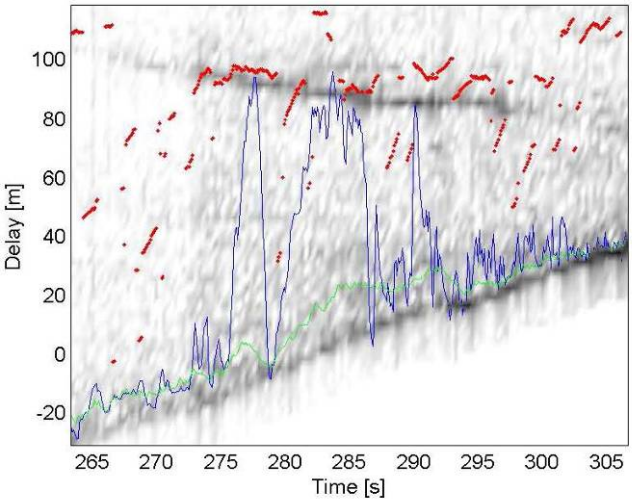


**Figure 14: Direct comparison of particle receiver, and NC-DLL – example: Echo with shadowed LOS.**

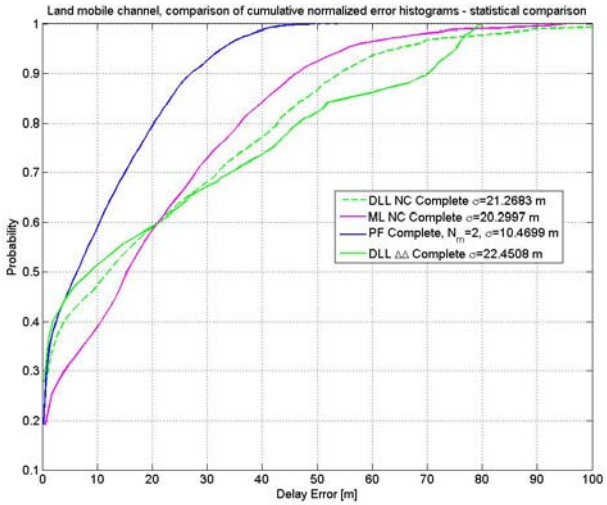


**Figure 15: Direct comparison of different receivers using a GPS C/A signal.**

## THE MULTIPATH CHANNEL'S IMPACT ON TRACKING OF DIFFERENT SIGNALS

Four different GNSS signal types were simulated: Two of them in the L1 frequency band and two of them in Galileo's E5 band. Specifically, the simulations were run with the GPS C/A code signal (BPSK(1)), the Galileo BOC(1,1) signal, the AltBOC(10,10) signal using its full bandwidth, and a BPSK(10) signal which uses the E5b frequency band.

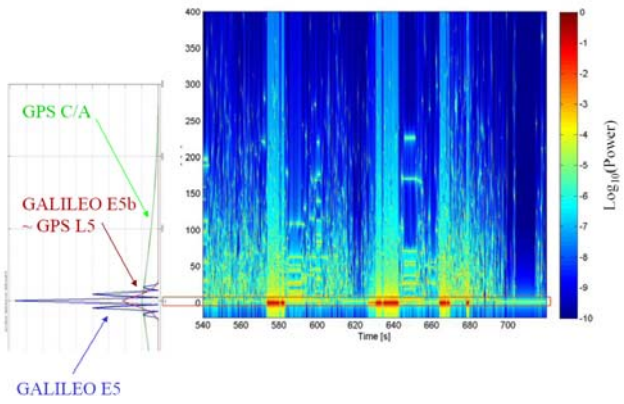


**Figure 16: The simulated channel impulse response as generated by the DLR land-mobile urban channel model.**

The channel impulse response which was used for the simulations is reported in Figure 16. This channel represents a challenging situation: long periods with only little power alternate with short periods of a strong line-of-sight component. The delay of the line-of-sight signal

has been moved to τ=0s for every impulse response. The receiver is actually moving towards the transmitter, which can be seen as decreasing delay in the plots with the tracking results for the four respective signals, Figure 17 to Figure 20.

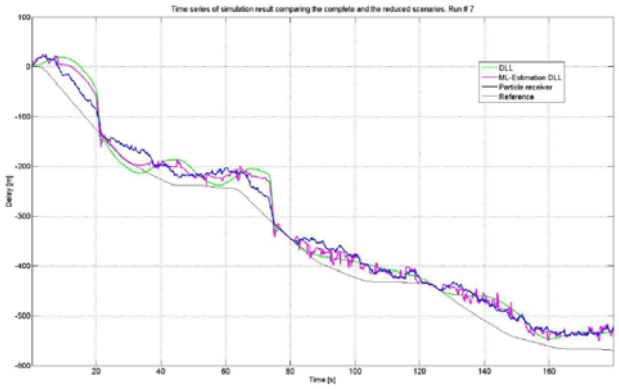


**Figure 17: Pseudorange estimation for GPS C/A code signal tracking using the three employed receiver algorithms.**

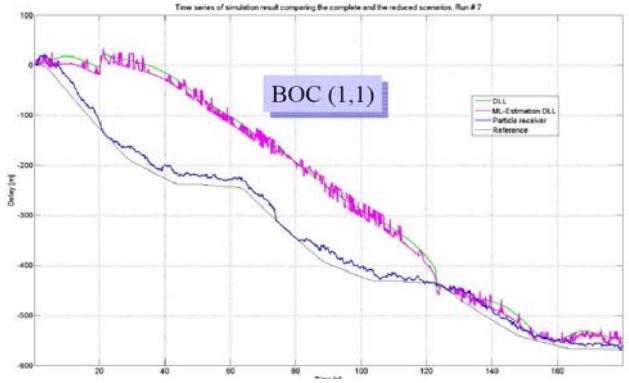


**Figure 18: Pseudorange estimation for BOC(1,1) signal tracking using the three employed receiver algorithms.**

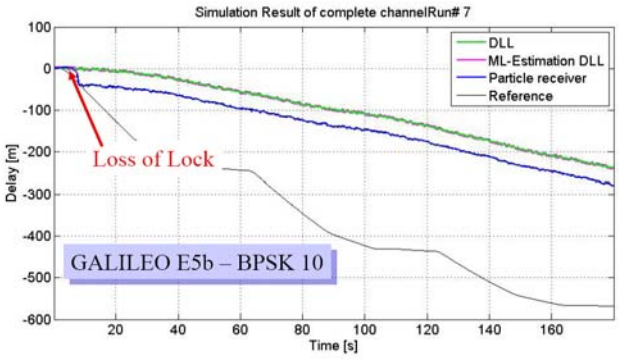


**Figure 19: Pseudorange estimation for BPSK(10) signal tracking using the three employed receiver algorithms.**

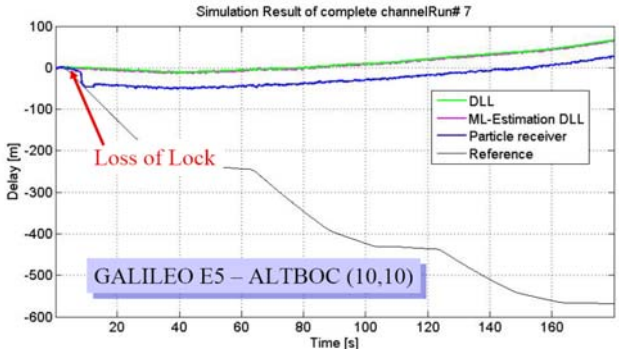


**Figure 20: Pseudorange estimation for AltBOC(10,10) wideband signal tracking using the three employed receiver algorithms.**

The C/A code signal and the BOC(1,1) signal tracking meets the challenge of the difficult channel conditions. Although, of course, the navigation error is increased in periods where the LOS is shadowed the receiver is able to track the signal robustly.

Yet it turned out that the wideband signals lost lock very often than the narrowband signals. The loss of lock happens usually in a situation where the LOS is obstructed. Assuming that the DLL is perfectly synchronized, the correlators are acting as a filter with the impulse response being the signal in space itself. Result of filtering a GNSS signal with this filter would be its autocorrelation function. It should be mentioned that we used a generic receiver that did not reacquire the signal after a loss of lock nor it detected the loss of lock.

We plotted the autocorrelation functions of the different signals in Figure 16 in the same scale as the channel impulse response. The trivial fact that a higher chip rate leads to a narrower autocorrelation function shall be mentioned. This results in the capability of the wideband signal to suppress multipath reflections better than the narrow band signals.

According to [5] the output of a correlator at time $t$ with lag $\tau$ can be written as

$$C(t,\tau) = \frac{1}{T_c}\sum_{i=0}^{N} a_i(t)\cdot\varphi_{ss}(\tau-\tau_i(t))$$

if the channel parameters are assumed to be constant within the correlation interval. The number of multipath components is denoted by $N$, the complex weight of each component is given by $a_i(t)$ and their delay is given by $\tau_i(t)$. The signal's autocorrelation function is given by $\varphi_{ss}(t)$. If the autocorrelation function of a specific signal $\varphi_{ss}(\tau_1)=0$ for a given multipath component delay $\tau_1(t_1)$, this component is filtered out and does not contribute to the correlation result anymore.

This explains why a wideband signal has the – intended – capability to suppress near echoes much better than its narrowband counterparts.

This advantage of filtering of multipath reception in situations where the LOS is present is obvious but converts into a disadvantage where the LOS is shadowed. Now the correlators are filtering out all the echoes. Additionally, since the LOS is no longer present the DLL is losing lock caused by a lack of signal power.
Narrowband signals still gather the power provided by multipath components with larger delay. In Figure 16 the red box shows the part of the channel being used by the E5 signals main lobe. The picture illustrates very well the amount of multipath energy that is filtered out by the E5 signal in contrary to the GPS C/A code signal.

This tradeoff between robustness and accuracy seems to be valid independently of the signal itself: Wideband signals are in general more accurate in LOS conditions but are less robust in obstructed situations. The narrow band signal is more robust in obstructed situations since it can use the power of the reflections for tracking but its accuracy is in general lower.

**Direct comparison of GPS C/A vs. BOC (1,1)**

The direct comparison between GPS C/A and GALILEO BOC (1,1) is shown in Figure 21. It can clearly be seen that for any receiver being simulated the use of BOC (1,1) results in more accurate results than for GPS C/A. It shall be mentioned that also the BOC (1,1) is less robust than the GPS C/A signal. But due to the small difference in bandwidth this reduced robustness ins only minor. The BOC (1,1) is robust enough to keep synchronized in most of the shadowed situations.

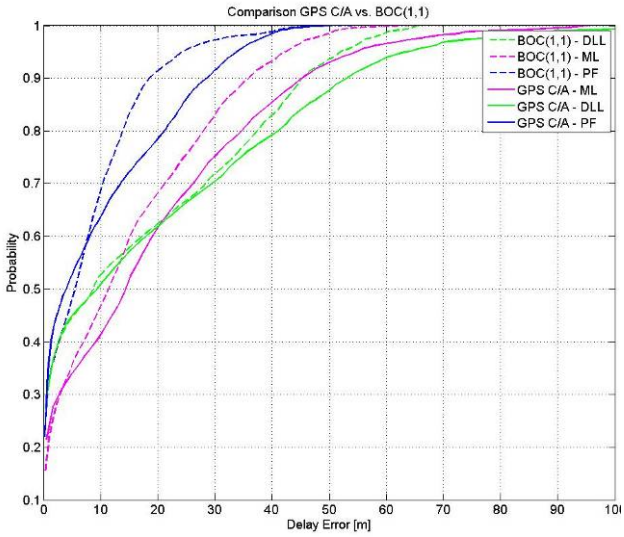


**Figure 21: Direct comparison between GPS C/A and BOC (1,1)**

**CRITICAL RECEIVER SITUATIONS**

During this activity we have identified critical situations for DLL based receivers. Figure 22 shows a situation where the DLL based receivers lost lock.

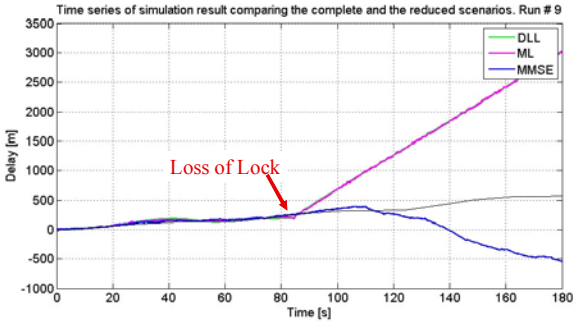


**Figure 22: Loss of lock situation in an urban environment**

Figure 23 is showing the channel impulse responses during this event. It is peculiar that at the moment of loosing lock the channel state changes severely. During nearly the whole segment the channel is shadowed but only during the seconds 73-75 and 85 - 87 the line of sight comes through for a short moment. We name this phenomenon "Short line of sight hit" or SLOSH for short. To understand the reaction of the receiver Figure 12 shows its structure. As being a classical DLL the early-late detector is realized as a standard narrow correlator. It shall be mentioned that the detector output is not divided by the signal amplitude to prevent zero forcing. The main correction elements are realized in two integrators one as a PI-element and one as an integrator. While the LOS is shadowed the receiver get low correction outputs from the detector. It can track the signal with a quite high but for the given channel conditions reasonable error during the shadowing period. Then at second 73 the LOS hits the receiver and suddenly the E/L-detector is generating a big output. If the LOS would stay present over a longer period the receiver would be set properly on the correct delay. But since the LOS disappears quickly after two seconds the DLL is not in a steady stay. Unfortunately the big output during the SLOSH has been fed into the integrators and has been accumulated there. Now the correction output of these integrators is mainly driven by the input during the SLOSH since the correction signal after it is again very weak. This behavior can clearly be seen in Figure 24. from second 75 the estimated delay is deviating constantly from the correct value. Now in second another SLOSH hits the receiver. Again when the LOS reappears the detector output is huge since the offset is large and the correlator outputs are big. The DLL tries immediately to correct its estimate to the corrected value. And again before reaching a steady

state the LOS disappears. And again the receiver is executing the last command stored in the integrators since again the detector output is weak. As a final result the DLL is loosing lock quickly.

We consider the SLOSH as a critical situation for a DLL especially if it occurs as a double feature. The "flywheel effect" of the integrators are misleading the DLL severely after the LOS disappears. Interestingly this effect is not happening for a particle receiver since this receiver judges its estimates directly with the current measurements. There are no integrators necessary in this concept that could mislead the receiver.

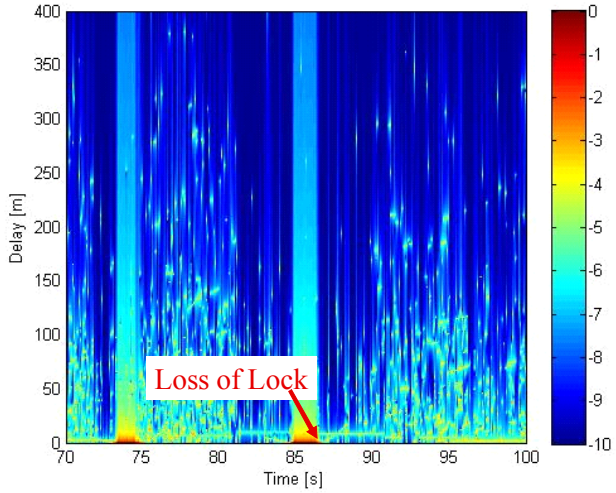


**Figure 23: Channel impulse response plot for the loss of lock situation.**

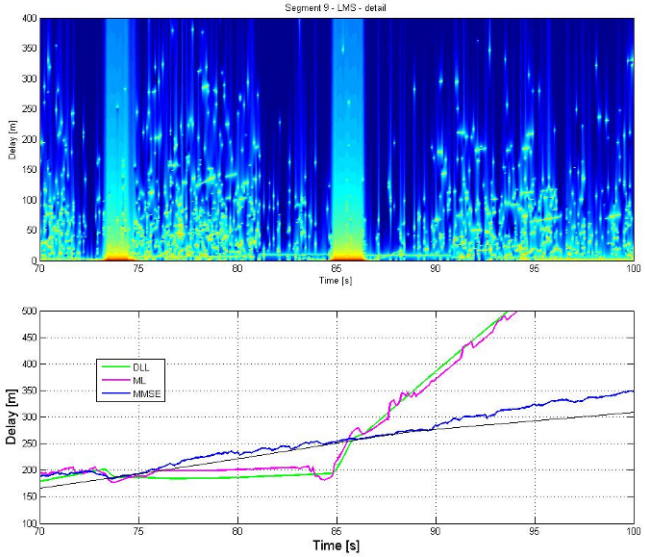


**Figure 24: The loss of lock situation in detail: Excerpt from Figure 22 and Figure 23 in the same time scale.**

## ACKNOWLEDGMENTS

The work reported in this paper has been supported under a contract of the European Space Agency in the frame of the European GNSS Evolutions Programme. The views presented in the paper represent solely the opinion of the authors and should be considered as R&D results not necessarily impacting the present EGNOS and Galileo system design.

## REFERENCES

[1] A. J van Dierendonck, P. Fenton, T. Ford, "Theory and Performance of Narrow Correlator Spacing in a GPS Receiver," Journal of The Institute of Navigation, Vol. 39, No.3 Fall 1992

[2] L. Garin, F. van Diggelen, and J. Rousseau, "Strobe and Edge correlator multipath mitigation for code," in Proceedings of the 9th International Technical Meeting of the Satellite Division of the Institute of Navigation (ION GPS 96), Kansas City, Missouri, USA, 1996, pp. 657–664.

[3] R. D. J. van Nee, J. Siereveld, P. C. Fenton, and B. R. Townsend, "The Multipath estimating delay lock loop: approaching theoretical accuracy limits," in Proceedings of the IEEE Position Location and Navigation Symposium (PLANS 94), Las Vegas, Nevada, USA, Apr. 1994, pp. 246– 251

[4] M. Lentmaier, B. Krach, P. Robertson, T. Thiasiriphet, "Dynamic Multipath Estimation by Sequential Monte Carlo Methods," in Proceedings of the 20th International Technical Meeting of the Institute of Navigation Satellite Division (ION GNSS 2007), Fort Worth, Texas, USA, Sept. 2007, pp. 1712-1721.

[5] Frank M. Schubert, Thomas Jost, Patrick Robertson, Roberto Prieto-Cerdeira, and Bernard H. Fleury: Evaluating Tracking Performance And A New Carrier-to-Noise Estimation Method Using SNACS, Position Location and Navigation System Conference (PLANS 2010), Palm Springs, California, USA

[6] Steingass A., Lehner A.: "Measuring the navigation multipath channel a statistical analysis", ION GPS 2004 Conference Long Beach, California USA, September 2004.

[7] A. Steingaß, A. Lehner, "A channel model for land mobile satellite navigation", European Navigation Conference ENC-GNSS 2005, Munich, (2005).